Energy Science & Engineering

ORIGINAL ARTICLE OPEN ACCESS

Forecasting Shifts in Europe's Renewable and Fossil Fuel Markets Using Deep Learning Methods

Yonghong Liu[1] | Muhammad S. Saleem[2] | Javed Rashid[3,4] | Sajjad Ahmad[2] | Muhammad Faheem[5,6]

[1]School of Computer Science, Chengdu University, Chengdu, China | [2]Department of Mathematics, University of Okara, Okara, Pakistan | [3]MLC Research Lab, Okara, Pakistan | [4]Information Technology Services, University of Okara, Okara, Pakistan | [5]School of Technology and Innovations, University of Vaasa, Vaasa, Finland | [6]VTT Technical Research Centre of Finland Ltd., Espoo, Finland

Correspondence: Muhammad Faheem (muhammad.faheem@uwasa.fi)

Received: 24 June 2024 | **Revised:** 4 October 2024 | **Accepted:** 30 October 2024

Funding: The authors received no specific funding for this work.

Keywords: Bi-GRU | European countries | internet of energy things | nonrenewable energy | renewable energy | smart grid

ABSTRACT

Accurate forecasts of renewable and nonrenewable energy output are essential for meeting global energy needs and resolving environmental issues. Energy sources like the sun and wind are variable, making forecasting difficult. Changes in weather, demand, and energy policy exacerbate this unpredictability. These challenges will be addressed by the bidirectional gated recurrent unit (Bi-GRU) model, which forecasts power-generating outcomes more efficiently. The investigation is done over a health data set from 2000 to 2023, including the energy states of the United Kingdom, Finland, Germany, and Switzerland. The comparison of our model (Bi-GRU) performance with other popular models, including bidirectional long short-term memory (Bi-LSTM), ensemble techniques combining convolutional neural networks (CNN) and Bi-LSTM, and CNNs, make the study more interesting. The performance remains better with a mean absolute percentage error (MAPE) of 2.75%, root mean square error (RMSE) of 0.0414, mean squared error (MSE) of 0.0017, and authentify that Bi-GRU performs much better than others. This model's superior prediction accuracy significantly enhances our ability to forecast renewable and nonrenewable energy outputs in European states, contributing to more effective energy management strategies.

1 | Introduction

The sources of energy include the sun, wind, and water, among others, which, apart from freeing us from fossil fuels, can supply all our current and future needs. For this reason, they are important to success in the long run [1]. Renewable energy is used in the production of electricity and the heating and cooling of structures. Conversely, nonrenewable energy sources like fossil fuels, natural gas, and coal, as shown in Figure 1, are finite in supply and have detrimental impacts on the ecosystem due to emissions and habitat destruction [2]. While such resources remain popularly used to produce electricity and power transportation systems, their environmental costs illustrate why we must quickly move toward more sustainable energy solutions.

European nations are taking aggressive steps towards meeting their climate targets and growing energy demands, investing heavily in renewables while managing nonrenewables carefully for maximum energy security and reduced environmental impact. With an ambitious target of reaching 100% carbon-neutral generation by 2050, the United Kingdom aims to produce 43% of its electricity from renewable sources such as wind, solar, hydropower, and bioenergy by 2020. The United Kingdom continues its leadership in renewable energy generation, setting new records every year since reaching 138 terawatt-hours of zero-carbon generation in 2022. Through this change, the United Kingdom is moving away from traditional nonrenewable energy sources like nuclear power, coal, and fossil fuels [3]. Nuclear energy will account for more than 40% of

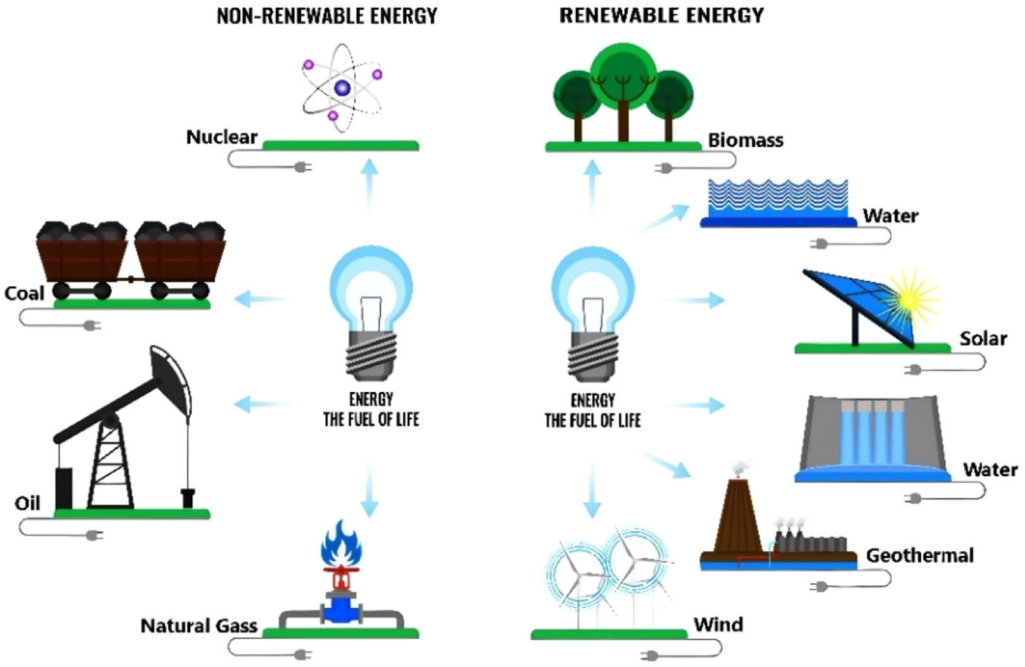

FIGURE 1 | Sources of renewable and nonrenewable energies.

Finland's electricity generation in 2023; wind and hydroelectricity will account for approximately 19% of the total. Although nuclear energy remains the predominant energy source, the nation has witnessed significant advances in renewables, resulting in a significantly decarbonized electricity industry [4]. Germany outshines government expectations regarding renewable energy use, with an unprecedented 59.7% of net electricity generation coming from renewable sources such as wind power (32%), hydropower (5.9 TWh), and solar panels producing over 59%. Germany continues to use hard coal and lignite, yet generation has decreased by 35% and 27% as part of their push towards reaching net zero emissions by 2050 [5]. Switzerland's low-emission electricity grid mainly relies on nuclear energy due to hydropower accounting for around 60% of energy output and photovoltaics rapidly expanding, both of which contribute towards maintaining low emissions levels. Switzerland has made impressive strides toward decoupling energy consumption from economic development. However, its policies must align fully with its 2030 emission reduction targets due to its reliance on imported natural gas, nuclear power, and oil [6].

Pollution and inflation rise with population expansion. Thus, nonrenewable and renewable energy sources are needed to meet electrical demand [7]. As a result, power output projection models must be made to predict what will be needed accurately. It will allow for cheap, long-lasting energy solutions that meet current energy needs and protect the environment for future generations.

Deep learning is the process of identifying complex patterns in large data sets by using artificial neural networks. It can assist with computer security in addition to weather prediction. Accurate forecasting of future production and consumption is essential for both nonrenewable and renewable energy sources using this method. More advanced models, such as Bi-GRUs [8] and Bi-LSTM [9], may assist in improving prediction accuracy. Since these technologies provide program managers and energy-efficient project managers access to dependable data, they may be advantageous to their efforts [10]. These models are necessary if we want to determine what proportion of the energy mix is derived from nonrenewable and renewable sources. Its assistance makes both grid maintenance and the switch to renewable energy sources less complicated.

For better energy use, deep learning helps predict how much power will be made. This was looked into for 2 years by Venkateswaran and Cho [11]. They used their novel hybrid deep learning model, SSA-CNN-LSTM, to forecast solar power in greenhouses more accurately than other models. In singular spectrum analysis (SSA), the reconstructed time series S_t is obtained by adding the individual components C_i:

$$S_t = C_1 + C_2 + C_3 \ldots\ldots C_i. \tag{1}$$

Unsal et al. [12] assess Turkey's potential for renewable energy using machine learning approaches, including light gradient boosting machine (LightGBM), gradient boosting regression (GBR), and random forest (RF), in conjunction with neural networks such as artificial neural networks (ANNs), LSTM, CNN, and hybrid CNN-LSTM models. LightGBM performs better than the other methods in terms of accuracy. Photovoltaic (PV) cell voltage in mathematical modeling can be computed using:

$$V = \frac{nkT_C}{q}\mathrm{Ln}\left(\frac{I_L + I_D - I}{I_D}\right) - IR_s. \tag{2}$$

In Cen and Lim [13], present PatchTCN-TST, a unique multitask learning model that significantly improves accuracy over conventional techniques and helps with demand-side management

for net-zero emissions in buildings by efficiently forecasting short-term multiload energy use. The temporal convolutional network (TCN) block employs causal convolution, meaning that the only mapping from the elements of time t and past t is what is produced at time t. The following defines the weight normalization and causal convolution operation at time t:

$$G(t) = (x^{*}g)(t) = \sum_{j=0}^{k-1} g(j) \cdot x_{t-j}.$$
$$w_{\text{norm}} = \frac{w}{\|v\|} h. \tag{3}$$

Motwakel et al. [14] built an MDLFM-ECP tool using LSTM, Bi-LSTM, deep belief networks (DBN), GRU, and chaotic cat swarm optimization (CCSO). This tool improves renewable and nonrenewable energy prediction with a minimal MAPE of 3.58%.

This study aims to address the significant gaps in research on forecasts of renewable and nonrenewable power output. Specifically, it focuses on filling the gaps in the data set related to electricity generation in European countries. Optimizing the use of this information is essential since any mistakes in the data might result in substantial forecast errors, which can hurt energy sector planning and regulation. This study identifies deficiencies in correctly predicting renewable and nonrenewable power generation. Specifically, it focuses on improving the accuracy of long-term predictions and reducing inaccuracies for strategic planning purposes. The statement underlines the innovative approach of employing more advanced models, such as Bi-GRU, to accurately predict future trends until 2030.

The main contribution of this work is as follows:

- This work presents the Bi-GRU model, enhancing the precision of predictions for renewable and nonrenewable power generation.
- This study uses Bi-GRU layers to record relationships between times in both directions, changes the input dimensions on the fly for different datasets, scales each country's data separately with MinMaxScaler, and has a flexible, scalable design that makes it easy to combine different and larger datasets.
- In this study, an updated data set is used until 2023 for the total electricity generation from renewable and nonrenewable sources in European countries. It aims to improve the precision of long-term forecasts for renewable and nonrenewable electricity and reduce prediction errors, thereby reducing the likelihood of mistakes in planning.
- This study contributes by forecasting total renewable and nonrenewable electricity generation until 2030.

The subsequent section of the article will be structured as follows: Section 2 contains a literature review. Section 3 covers several aspects, including materials, data set splitting, data processing, the suggested model (Bi-GRU), experimental design, and assessment measures. Section 4 includes a model comparison and an evaluation of past research in the context of the results and comments. Section 5 of the report contains the conclusion and a future strategy.

2 | Literature Review

The use of deep learning algorithms has revolutionized energy forecasting, enhancing the prediction capabilities for both renewable and nonrenewable power generation. Models like CNNs and recurrent neural networks (RNNs) are particularly effective in medium-term forecasting, demand response, error detection, and identifying hidden patterns in energy production. These capabilities allow for improved reliability, better resource allocation, and more accurate forecasts [10, 15]. Although these advantages exist, the larger issues in long-term energy planning are not always well addressed by the models currently in use, particularly when it comes to integrating intermittent and continuous energy sources.

European nations have placed great emphasis on renewable energy sources in an effort to become less dependent on fossil fuels. This push has underscored the importance of advanced forecasting models. However, many current models, while effective for specific types of energy or short-term predictions, fail to comprehensively integrate both renewable and nonrenewable energy outputs for long-term predictions. For instance, Al-Ali et al. demonstrated the effectiveness of hybrid CNN-LSTM-Transformers in forecasting solar energy production, showing superior accuracy compared to traditional methods. Still, their focus remains limited to a single energy source [16]. Similarly, Alrasheedi et al. improved short-term load predictions on Saudi smart grids using hybrid deep learning models, but the study only focuses on short-term forecasting [17].

Efforts to integrate multiple energy sources for forecasting have seen some advancements. Anu Shalini et al. [18] combined solar and wind energy sources using a CNN-based Bi-LSTM model to forecast energy production. While promising, this approach is restricted to specific applications and lacks generalization across broader datasets. Mystakidis et al. applied machine learning techniques to improve renewable power output forecasting and help distribution system operators manage demand response [19]. Yet, the study does not address the complexities of forecasting when both renewable and nonrenewable sources are involved. Nikulins et al. integrated solar and wind power with hydrogen production using artificial intelligence-powered frameworks. However, their approach focuses narrowly on niche applications, limiting its utility for broader energy forecasting [20]. Kumar et al. [21] achieve a mean squared error of only 1.36, representing a significant improvement in renewable energy estimation accuracy through fully linked and convolutional neural networks. However, their approach primarily focuses on short-term forecasting in microgrids, which may limit its applicability to long-term energy management strategies. Similarly, a novel technique, PVMD-ESMA-DELM, employs deep extreme learning machine modeling with an enhanced slime mold algorithm and particle swarm optimization to optimize renewable power output projections [22]. While this technique shows promise, its complexity may hinder implementation in real-time forecasting applications.

Pasandideh et al. [23] analyze wind power data and population diversity, providing a feasible path forward for renewable energy forecasting. However, the study's exclusive focus on wind energy limits its broader applicability by ignoring the intricate structure of energy production. SSA-CNN-LSTM, a hybrid deep learning model developed by Venkateswaran and Cho, leverages spatial and temporal correlations to reliably anticipate solar power output in greenhouses [11]. However, because their method was created specifically for greenhouse conditions, it may only work in some settings or with other types of energy.

Accurate hourly green power production forecasting is critical in urban settings. Bi-LSTM models with min-max normalization provide a minimum MAPE of 7.7256%, as shown by Wibawa et al. [24]. However, the reliance on normalization techniques may overlook important temporal dynamics in energy consumption patterns. Marques et al. [25] point out that deep learning methods are becoming increasingly popular in solar energy forecasting. They demonstrate that LSTM-GRU is a good strategy for developing sustainable energy in the Amazon Basin. However, since their study is restricted to certain geographic settings, it could not adequately represent the difficulties associated with energy forecasting in numerous regions.

Even while this research shows the promise of several deep learning models, there are still a lot of holes and restrictions. Many of the models that are now in use ignore the difficulties of combining many energy types and long-term forecasts in favor of concentrating just on certain renewable energy sources or short-term forecasting. Abubakar et al. [26], for instance, use LSTM to improve the accuracy of solar power production in smart grids, obtaining a remarkable 97%. Their results, however, could not adequately represent the complex interrelationships between different renewable and nonrenewable sources, which would restrict their use for thorough energy forecasting. In a similar vein, Unsal et al. [12] determine that LightGBM is the most accurate model for predicting renewable energy in Turkey; however, their research needs to account for a wider variety of energy outputs or tackle the particular difficulties associated with predicting across borders. Akhter et al. [27] boost renewable energy production by employing an RNN-LSTM model to estimate hour-ahead PV power and optimize output prediction for multiple PV plant technologies. Since it largely relies on short-term estimates, their study may have missed long-term energy production trends. This narrow focus limits the model's energy planning potential.

The Bi-GRU model presents a possible remedy for the above problems. The Bi-GRU model is distinct in that it takes both directions of the data into account. As a result, it can comprehend the complex temporal relationships necessary for trustworthy forecasts in the far future. Due to its bidirectional processing capabilities, the model is an ideal tool for several European nations attempting to integrate renewable and nonrenewable energy sources. It excels at deciphering hierarchical links seen in long-term datasets. By enhancing prediction accuracy and decreasing error rates until 2030, this study will aid strategic energy planning efforts by using the Bi-GRU model. Table 1's contents are significant.

3 | Materials and Methods

This section describes how we collected and processed the data for our study. It also provides the working and design of the proposed model (Bi-GRU). The following research flow provides a detailed summary of the methodologies used in our investigation, as seen in Figure 2.

3.1 | Data Set

Our data set illustrates the evolution of renewable and nonrenewable energy sources from 2000 to 2023 in four European countries—the United Kingdom, Finland, Germany, and Switzerland. A comprehensive analysis spanning these nations allows for an in-depth study encompassing diverse geographic regions, energy landscapes, and policy approaches providing deep insight into renewable and nonrenewable energy dynamics. It compares total renewable electricity production (TREP) and total nonrenewable electricity production (TNREP) across four European nations in a comparative manner. This statistic breaks down renewable energy production into four categories: bioenergy, solar energy, hydropower, and other renewable and nonrenewable energy sources: nuclear power, fossil fuels, and other nonrenewable resources, all expressed as gigawatt-hours (GWh). The data set from 2000 to 2021, obtained initially from a source [28], and from 2022 to 2023, obtained from [29], details both total renewable energy production figures and total nonrenewable energy production numbers, as reported in Table 2. It illustrates each nation's contribution to producing renewable and nonrenewable electricity within Europe. These countries were chosen due to their diverse geographic locations, energy policies, and significant contributions to Europe's renewable and nonrenewable energy sectors, which provided us with an in-depth view of energy transition and sustainability efforts across Europe. They were chosen to shed light on trends and patterns within Europe's energy output.

3.1.1 | Data Preprocessing

At our start-ups, we meticulously handle a substantial amount of data. Our deep learning and data science engineers perform the crucial task of ensuring the usability of datasets for model training. Our knowledge of biogas, solar energy, hydropower, and other forms of renewable energy must be accurate and dependable. It stands in opposition to data about fossil fuels, nuclear power, and other forms of nonrenewable energy. Identifying and resolving data inaccuracies, missing statistics, and other issues in these critical energy domains requires a comprehensive examination. Before training, data originating from various energy sources, such as electricity, solar energy, biofuel, and others in gigawatt-hours, must undergo thorough cleansing. Cleaning up the data is essential for making sure that comparisons of the overall amount of green and nonrenewable energy are correct. It gives a strong foundation for training models and produces valuable results.

After cleaning a data set, column numbers must be consistent across rows. Equation (4) shows that min-max normalization achieves this goal. Limiting the data to 0–1 reduces the

TABLE 1 | An overview of related literature.

[Reference], Year	Methodology	Country	Accuracy/error	Cons
[12], 2024	LightGBM	Turkey	RMSE: 1.7479, MAE: 1.1072	The sole emphasis is on renewable energy.
[16], 2023	CNN-LSTM-Transformer	Finland	RMSE: 0.344, MAE: 0.393	The exclusive attention is on only solar energy.
[17], 2022	CNN-GRU, CNN-RNN	Saudi Arabia	RMSE: 77.4877 (Jeddah)RMSE: 20.7501 (Madinah)	The sole emphasis is on renewable energy.
[18], 2023	CNN based BILSTM	India	MSE: 0.0884, MAE: 0.0219, R^2: 0.9931256 (solar power)MSE: 2.1432, MAE: 1.0125, R^2: 0.9920 (wind power)	The exclusive attention is on renewable energy.
[19], 2023	Ensemble Approach	Cyprus	RMSE: 1.9993, MAE: 0.8306, MSE: 3.9972, R^2: 0.8913	The sole emphasis is on renewable energy.
[20], 2024	FCN, CNN	Latvia	MSE: 1.77 (FCN)MSE: 1.36 (CNN)	The primary focus is on solar and wind power.
[21], 2021	LSTM-RNN	—	RMSE: 4.45 (solar power) RMSE: 0.17 (wind power)	The primary focus is on solar and wind power.
[22], 2022	PVMD-ESMA-DELM	China	MAE: 0.9709, MAPE: 0.0272RMSE: 1.4188, R^2: 0.9713	The exclusive focus is on wind power.
[23], 2024	LSTM	—	RMSE: 0.47.	The only focus is steam energy.
[11], 2024	SSA-CNN-LSTM	South Korea	MAE: 0.1202 (1 h ahead), 0.1400 (2 h ahead), 0.1774 (day ahead)	The focus is solely on solar energy.
[24], 2024	Bi-LSTM	—	MAPE: 7.7256%, RMSE: 0.12346, R^2: 0.6151	The sole emphasis is on renewable energy.
[25], 2024	MLPLSTM2LST-M-GRU	Brazil	MLPMAE: 0.61, MAPE: 19.5, RMSE: 1.05LSTM2MAE: 0.81, MAPE: 22.77, RMSE: 1.05LSTM-GRUMAE: 0.89, MAPE: 19.2, RMSE: 0.75	All attention is focused on solar energy.
[26], 2024	RNN, LSTM, GRU	—	LSTMRMSE: 65.892, MAE: 41.0046	The focus is solely on solar energy.
[27], 2022	RNN-LSTM	Malaysia	RMSE: 26.85, 19.78, 39.2, R^2: 0.995, 0.9943, 0.996	The spotlight is on photovoltaic PV.

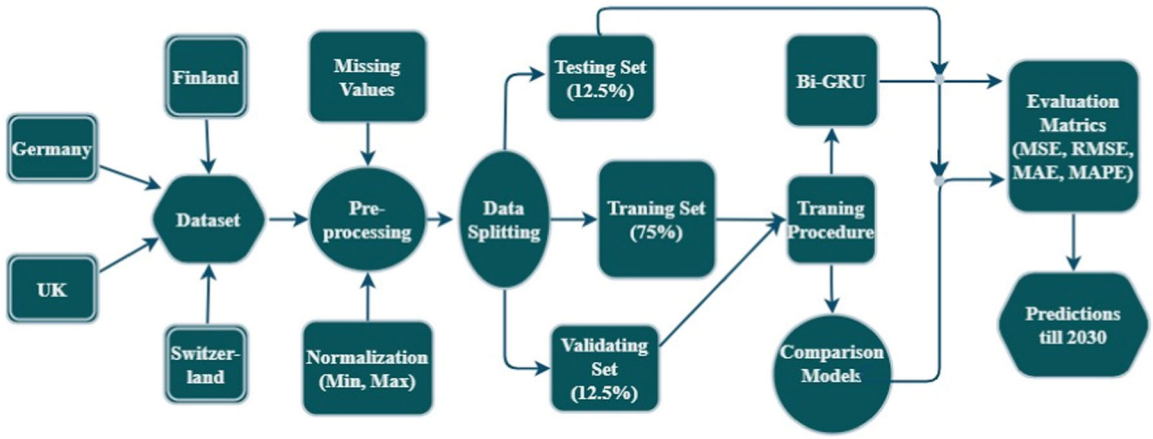

FIGURE 2 | Research flow.

TABLE 2 | Renewable and nonrenewable electricity (GWh) production data set.

Years	Country	Bio-energy	Solar energy	Hydro-power	Other renewable energy	TREP	Fossil fuels	Nuclear energy	Other nonrenewable energy	TNREP
2000	UK	3936	1	5086	947	9988	278,823	85,063	3213	367,099
2001	UK	4526	2	4056	965	9840	280,205	90,094	4942	375,241
2002	UK	5081	3	4787	1256	11,156	282,756	87,848	5516	376,120
—	—	—	—	—	—	—	—	—	—	—
—	—	—	—	—	—	—	—	—	—	—
2023	UK	33,850	13,510	5230	354,770	407,360	117,150	41,290	117,150	275,590
2000	Finland	8639	1.576	14,660	78	23,370.58	23,855	22,479	263	46,597
2001	Finland	8270	1.715	13,205	70	21,540.72	29,869	22,773	297	52,939
2002	Finland	8988	1.865	10,776	64	19,858.87	32,467	22,295	363	55,125
—	—	—	—	—	—	—	—	—	—	—
—	—	—	—	—	—	—	—	—	—	—
2023	Finland	11,070	650	15,110	105,290	132,120	4460	33,920	4460	42,840
2000	Germany	4331	60	21,732	9352	36,579	361,442	169,606	10,020	541,068
2001	Germany	4590	116	22,733	10,456	43,295	364,835	171,305	12,371	548,511
2002	Germany	5309	188	23,124	15,856	47,708	365,426	164,842	11,949	542,217
—	—	—	—	—	—	—	—	—	—	—
—	—	—	—	—	—	—	—	—	—	—
2023	Germany	46,020	61,560	19,480	609,660	736,720	231,480	8750	231,480	471,710
2000	Switzerland	842	11	36,835	3	37,692	1084	26,446	2298	29,828
2001	Switzerland	881	13	41,308	4	42,207	1092	26,811	2324	30,227
2002	Switzerland	916	15	35,168	5	36,104	1115	27,234	2676	31,025
—	—	—	—	—	—	—	—	—	—	—
—	—	—	—	—	—	—	—	—	—	—
2023	Switzerland	960	4190	38,550	74,810	118,510	1720	24,190	1720	27,630

influence of any one component on the outcome [30]. Outcomes ensure that all features contribute equally to model learning. Standardized feature columns including "bioenergy," "solar energy," "hydropower," "other renewable energy," "fossil fuels," "nuclear," and "other nonrenewable energy" assure size and distribution consistency during normalization. A detailed energy source comparison and analysis are performed at this level. The goal columns "total renewable energy" and "total nonrenewable energy" in GWh are handled equally to enhance model training and prediction accuracy. Table 3 shows the data set's normalized data.

$$S' = \frac{S - S_{min}}{S_{max} - S_{min}}, \tag{4}$$

S is the set of values; S′ is the normalized value of S, and S_{max} and S_{min} are the maximum and minimum values in S, respectively.

3.1.2 | Data Splitting

Splitting the data is essential for training and testing deep learning models. It is essential to keep the models from overfitting and to ensure they can be used in many situations [31]. Our study used data from four European countries: the United Kingdom, Finland, Germany, and Switzerland. The data from four European countries is split individually into training, validation, and testing. Records from 2000 to 2017 comprise the training data set, comprising roughly 75% of the total data, providing an essential background for training a model. A validation data set with data from 2018 to 2020, comprising 12.5%, serves to adjust parameters to avoid overfitting; testing records consisting of power generation from 2021 to 2023 also account for 12.5%; this allows us to assess model functionality against fresh, untested data sets (Figure 3 illustrates this method).

3.2 | Proposed Methodology

Deep learning models exist that can enhance prediction accuracy. Our study explores the problem with a Bi-GRU. This innovative method increases the precision of our predictions and is also proposed as part of this composite model. The novelty of this approach is that it leverages bidirectional GRU layers to find relationships in the future and backwards in time, which helps predict sequences by better understanding the context. It changes the input measurements on the fly to fit the predicted 3D shape for GRU layers, ensuring it works with a wide range of datasets. Using MinMaxScaler, the data from each country is scaled separately. It normalizes features and goals to make the training process better. The flexible and scalable design makes it easy to add support for bigger and more varied datasets. It can also handle datasets from multiple countries without any problems.

3.2.1 | Bi-GRU Neural Network Model

GRUs are a refined modification of the LSTM network that effectively and directly captures sequential or temporal information. GRUs employ two gates, the update gate and the reset gate, which operate using a distinct process compared to LSTM. For example, the update gate of the GRU combines the forget and input gates of the LSTM, but the reset gate remains unchanged. Like an LSTM network, a GRU model alters the information within its units, but it does not need separate memory cells, as seen in Figure 4.

Assume that y_t, v_t, r_t, $\hat{h}_t$, h_{t-1} and h_t represent, in that order, the current input, update gate, reset gate, candidate hidden state of the presently hidden node, hidden state at the prior instant, and current hidden state [8]. The update gate, v_t, may be expressed as follows: It establishes how much information from h_{t-1} will pass along to the future and formulates it as:

$$v_t = \sigma(W_{vy} y_t + U_{vh} h_{t-1}). \tag{5}$$

The W_{zy} and U_{vh} weights, found during algorithm training, are multiplied by yt and h_{t-1} in this case. The values of the two findings, which range from 0 to 1, are calculated by adding them together and running them through a sigmoid function. When the value is 0, the data remains in its current concealed state; otherwise, it forgets it. The reset gate, or r_t, determines the amount of historical data to discard and expresses it as follows:

$$r_t = \sigma(W_{ry} y_t + U_{rh} h_{t-1}). \tag{6}$$

Except for the weights and the gates, Equations (5) and (6) are the same for the update gate. The reset gate is used by the candidate hidden state of the presently hidden node, $\hat{h}_t$, to preserve pertinent historical data using:

$$\hat{h}_t = \tanh\ (W_{hy} y_t + r_t \odot U_{hh} h_{t-1}). \tag{7}$$

Here, y_t and h_{t-1} are multiplied by their W_{hy} and U_{hh} weights to get the Hadamard product ($\odot$), that is, the element-wise multiplication between r_t and $U_{hh} h_{t-1}$. To get $\hat{h}_t$, the output of these two stages is added together and run through a nonlinear activation function (tanh function). The last phase is to compute the hidden state that is now in place, h_t, by using:

$$h_t = (1 - v) \odot \hat{h}_t + v_t \odot h_{t-1.} \tag{8}$$

Equation (8) computes the Hadamard products (element-wise multiplications) between $(1 - v_t)$ and $\hat{h}_t$ and v_t and h_{t-1}. Their incapacity negatively impacts the accuracy improvement of unidirectional GRUs in concurrently analyzing historical and prospective data. The study used a Bi-GRU framework to achieve its goals; Figure 5 depicts a Bi-GRU model.

First, a forward GRU, $\overrightarrow{GRU}$, and a backward GRU, $\overleftarrow{GRU}$ simultaneously receive the input data sequence. At that moment, it will obtain the hidden state by concatenating the hidden states $\vec{h}_t$ and $\overleftarrow{h}_t$, which the forward and backward GRU generate at time t, respectively. This will yield the hidden state at that instant using Equation (9):

$$h_t = \text{concatenate}\ (\vec{h}_t, \overleftarrow{h}_t), \tag{9}$$

TABLE 3 | Normalized data set.

Years	Country	Bio-energy	Solar energy	Hydro-power	Other renewable energy	TREP	Fossil fuels	Nuclear energy	Other nonrenewable energy	TNREP
2000	UK	0	0	0.511	0	0	0.844	0.897	0	0.903
2001	UK	0.016	0	0.228	0	0	0.851	1	0.012	0.942
2002	UK	0.032	0	0.429	0	0.003	0.865	0.954	0.016	0.946
—	—	—	—	—	—	—	—	—	—	—
—	—	—	—	—	—	—	—	—	—	—
2023	UK	0.832	0.971	0.551	0.993	0.989	0	0	0.813	0.471
2000	Finland	0.070	0	0.674	0	0.038	0.515	0.016	0	0.415
2001	Finland	0	0	0.481	0	0.022	0.675	0.041	0.004	0.614
2002	Finland	0.135	0	0.158	0	0.007	0.744	0	0.013	0.683
—	—	—	—	—	—	—	—	—	—	—
—	—	—	—	—	—	—	—	—	—	—
2023	Finland	0.527	1	0.734	1	1	0	1	0.531	0.298
2000	Germany	0	0	0.747	0	0	0.781	0.990	0.004	0.794
2001	Germany	0.006	0.001	0.929	0.002	0.01	0.801	1	0.013	0.821
2002	Germany	0.021	0.002	1	0.011	0.016	0.805	0.960	0.011	0.798
—	—	—	—	—	—	—	—	—	—	—
—	—	—	—	—	—	—	—	—	—	—
2023	Germany	0.895	1	0.337	1	1	0	0	0.817	0.540
2000	Switzerland	0	0	0.568	0	0.064	0.462	0.827	0.217	0.735
2001	Switzerland	0.032	0.001	1.000	0	0.117	0.469	0.870	0.227	0.786
2002	Switzerland	0.061	0.001	0.407	0	0.046	0.489	0.919	0.359	0.887
—	—	—	—	—	—	—	—	—	—	—
—	—	—	—	—	—	—	—	—	—	—
2023	Switzerland	0.096	1	0.734	1	1	1	0.564	0	0.457

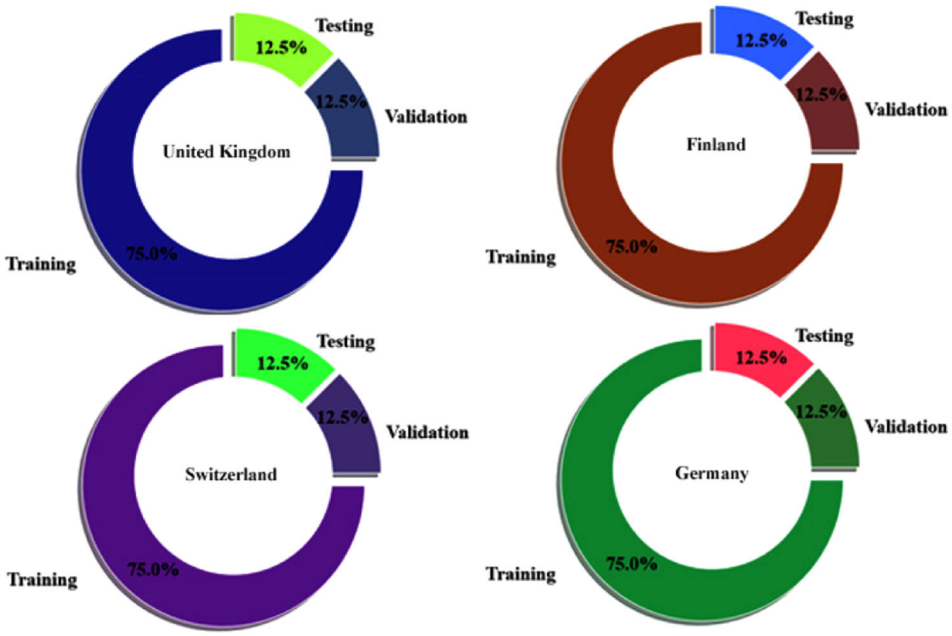

FIGURE 3 | Distribution of data.

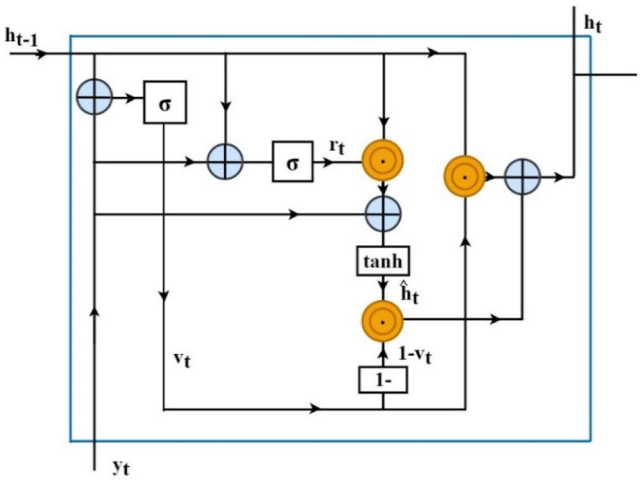

FIGURE 4 | Architecture of a GRU cell.

where $\vec{h_t} = \vec{\mathrm{GRU}}(h_{t-1}, y_t)$ and. $\overleftarrow{h_t} = \overleftarrow{\mathrm{GRU}}(h_{t+1}, y_t)$.

3.2.2 | Experimental Setup

A sequential neural network model is created in the present experiment to forecast the combined power generation from renewable and nonrenewable sources, measured in gigawatt-hours, in four European countries: the United Kingdom, Finland, Germany, and Switzerland. The model was specifically developed to analyze time-series data of different power sources and predict the overall electricity generation, divided into renewable and nonrenewable classifications. The neural network design comprises two bidirectional GRU layers, followed by two dense layers. To capture temporal relationships in both the forward and backward directions of the input sequence, the first 64-unit bidirectional GRU layer returns sequences. The training feature data set determines this layer's input form, time steps, and features. The next 64-unit bidirectional GRU layer bridges the more compact, fully connected layers and does not produce sequences.

After each repetition layer is added, a dense layer composed of 50 neurons is activated with rectified linear unit (ReLU). The nonlinearity allows the model to comprehend complex patterns in its input data more quickly. The final layer consists of a dense layer with a neuron count equal to the train target data set, representing the model's output for predicting total renewable and nonrenewable power production. This model is trained using the Adam optimizer and MSE loss function to minimize differences between anticipated and actual energy production values. This step completes 100 iterations of feeding the data set into a neural network to adjust and optimize model weights iteratively. Estimating total renewable energy uses input features like bioenergy, solar energy, hydropower generation, and other forms of renewable energy. At the same time, nonrenewable sources include fossil fuels, nuclear power, and nonrenewable forms of energy, such as other nonrenewable forms like oil and fossil energy production. These characteristics include all energy sources in each category, giving the model access to an extensive set of learning inputs. The model seeks to estimate renewable and nonrenewable energy output in gigawatt-hours for European nations, as indicated in Table 4.

3.3 | Evaluation Metrics

To assess the effectiveness of our method, we employed many assessment measures, including MAE, MSE, RMSE, and MAPE. The numbers in question are determined by Equations (10–13). The MAE quantifies the extent of the disparity between the observed and estimated values. The RMSE metric quantifies the extent of disparity between the observed and predicted values. The MSE quantifies the squared differences between observed and anticipated values. The MAPE quantifies the average

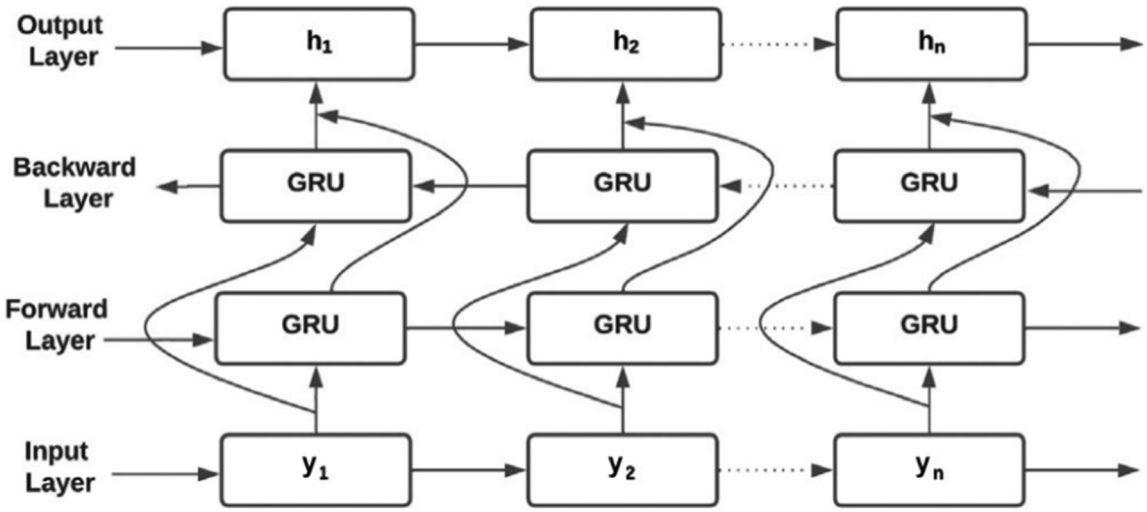

FIGURE 5 | Bi-GRU model.

TABLE 4 | Experimental setup of Bi-GRU model.

Component	Description
Model type	Sequential neural network
Layers	1. Bidirectional GRU (64 units)
	2. Bidirectional GRU (64 units)
	3. Dense (50 neurons, ReLU activation)
	4. Dense (output layer, linear activation for regression)
Optimizer	Adam
Loss function	MSE
Epochs	100

percentage difference between the observed and predicted values [32, 33].

$$\mathrm{MSE} = \frac{\sum_{l=1}^{m}(v_l - d_l)^2}{p}, \tag{10}$$

$$\mathrm{MAE} = \frac{\sum_{l=1}^{m}|v_l - d_l|}{p}, \tag{11}$$

$$\mathrm{RMSE} = \sqrt{\frac{\sum_{l=1}^{m}(v_l - d_l)^2}{p}}, \tag{12}$$

$$\mathrm{MAPE} = \frac{1}{p}\sum_{i=1}^{m}\left|\frac{v_i - d_i}{v_i}\right| \times 100, \tag{13}$$

where v_l is the actual power, d_l is the predicted power, and p is the number of values.

4 | Results and Discussion

Deep learning models are modeled and trained using Python and Keras tools. In contrast, training, validation, and testing steps occur through Google Colab [34], an environment offering robust graphic processing unit (GPU) support. Below are the main insights gained from this model:

1. We examined data from the renewable and nonrenewable electricity production database, which includes the United Kingdom, Finland, Germany, and Switzerland. We evaluated the Bi-GRU model's predictive and enhancing capabilities for renewable and nonrenewable power-generating methods.
2. The Bi-GRU model was directly compared to three other models: Bi-LSTM, CNN, and an ensemble model comprising both Bi-LSTM and CNN.
3. We conducted an ablation study on the European countries' data set.
4. We used the results of earlier studies to compare the Bi-GRU model's performance.

4.1 | Bi-GRU Model Performance on Datasets of Four European Countries

This section examines how well the Bi-GRU model predicts energy production in the United Kingdom, Finland, Germany, and Switzerland. Specifically, we check the model's predictions by comparing the power output from green and nonrenewable sources. The Bi-GRU model can accurately show energy production's complex time trends.

4.1.1 | Bi-GRU Model Performance on Data Set of United Kingdom

Using the United Kingdom data set and 100 iterations, Figure 6 displays the Bi-GRU model's training and validation losses as MSEs. It is a good match when validation loss decreases significantly before stabilizing, but training loss decreases significantly. After that, both losses decrease, but training losses are always less than validation losses. It means that learning is going well and could be better.

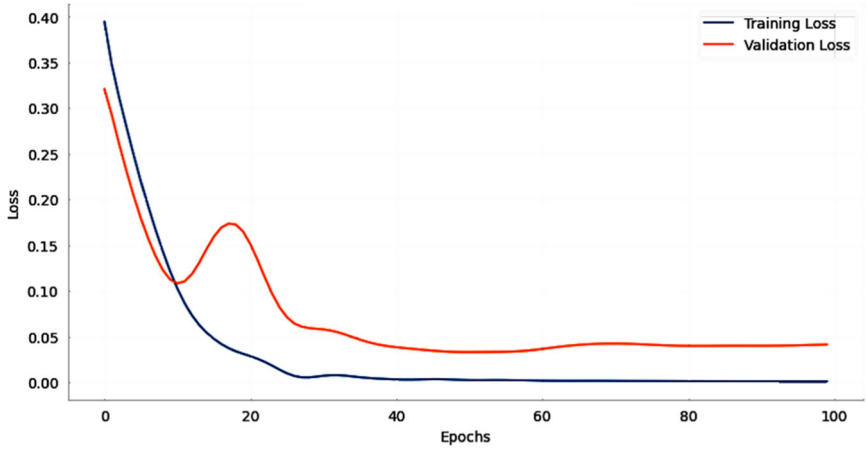

FIGURE 6 | Bi-GRU model's training and validation losses on the UK data set.

Table 5 shows how well a Bi-GRU model performed when tested on a UK data set. Three categories of error metrics are presented: The average squared prediction errors are represented by the MSE, which is 0.0064. The average absolute prediction errors are shown by the MAE, which is 0.034. The square root of the average squared errors is the RMSE, which is 0.0797. Additionally, the MAPE is 3.79%, which measures the average percentage error.

Table 6 presents forecasts for the United Kingdom's TREP and TNREP in normalized GWh from 2024 to 2030 using a Bi-GRU model. The normalized TREP starts at 0.621 in 2024 and shows a fluctuating decrease. In contrast, TNREP begins at 0.4 and exhibits a more significant drop by 2030, ending at 0.21.

Figure 7 shows a time series graph of the United Kingdom's TREP in normalized GWh from 2000 to 2030. TREP in the United Kingdom steadily increased from negligible levels in 2000 to a peak in 2019, followed by a slight dip in 2020. From 2021 to 2023, production experienced a notable fluctuation, reaching a peak in 2022. Predicted values from 2024 to 2030 show a gradual decline in production, suggesting a potential stabilization or even reduction in renewable energy output over the forecasted period.

Figure 8 illustrates the TNREP in the United Kingdom from 2000 to 2023, showcasing a gradual decline from 0.9032 to 0.4706 GWh, with a normalized decrease trend. The forecast anticipates TNREP fluctuations, peaking at 0.786 before declining to 0.21 by 2030. This trajectory suggests a notable transition from nonrenewable energy sources over the next 7 years.

4.1.2 | Bi-GRU Model Performance on Data Set of Finland

Figure 9 illustrates quick initial loss reductions for a Bi-GRU model using the Finland data set through a graph of MSE losses. The validation loss flattens out after a little bounce, but the training loss soon stabilizes, suggesting that the model learns well with some variation in generalization. Both losses stay steady and modest after around 20 epochs, indicating a well-fitted model.

TABLE 5 | Performance of Bi-GRU model on the UK testing set.

Error description	Error value
MSE	0.0064
MAE	0.034
RMSE	0.0797
MAPE (%)	3.79

TABLE 6 | Forecasting TREP and TNREP using the Bi-GRU model on the UK testing set.

Year	Normalized TREP in the United Kingdom	Normalized TNREP in the United Kingdom
2024	0.621	0.4
2025	0.777	0.354
2026	0.735	0.596
2027	0.728	0.304
2028	0.641	0.588
2029	0.59	0.572
2030	0.547	0.21

As can be seen from the low error rates in Table 7, the Bi-GRU model demonstrates strong predictive abilities on the Finland test set: an MSE of 0.0105 indicates high model accuracy, an MAE of 0.0475 indicates the model's average absolute deviation from the actual values is minimal, RMSE of 0.1023 indicates good predictive performance with reasonably low squared errors, and MAPE is 3.17%, which measures the average percentage error. Together, these measures indicate the model's resilience in producing accurate predictions.

Starting in 2024, Table 8 reveals a normalized TREP in Finland of 0.658 GWh and a normalized TNREP of 0.078 GWh. Over subsequent years, renewable energy production declined,

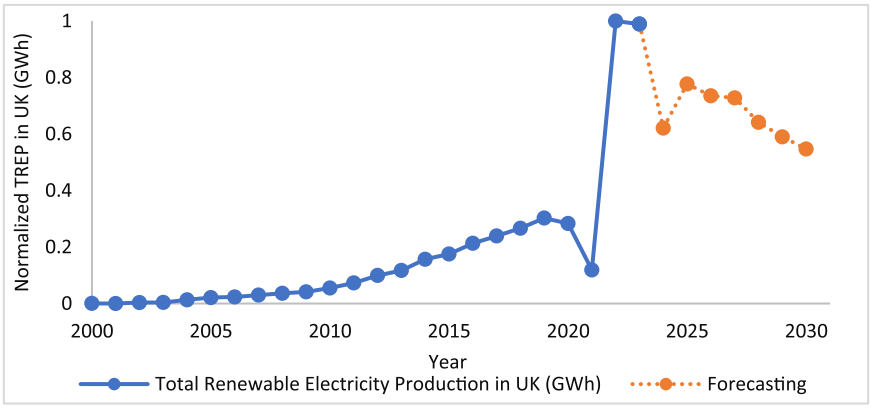

FIGURE 7 | Prediction of TREP in normalized form using the Bi-GRU model on the UK testing set.

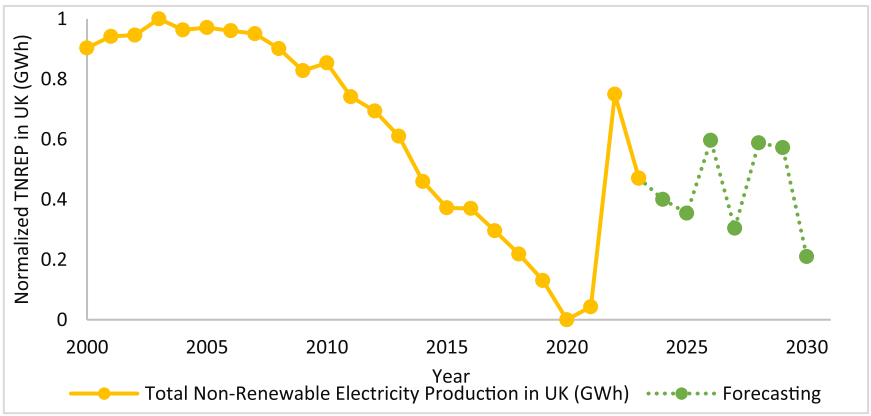

FIGURE 8 | Prediction of TNREP in normalized form using the Bi-GRU model on the UK testing set.

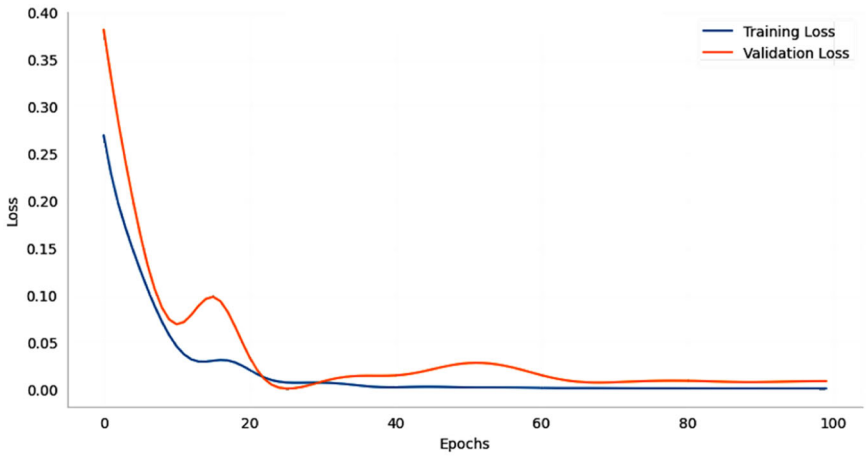

FIGURE 9 | Bi-GRU model's training and validation losses on the Finland Data set.

TABLE 7 | Performance of Bi-GRU model on the Finland testing set.

Error description	Error value
MSE	0.0105
MAE	0.0475
RMSE	0.1023
MAPE (%)	3.17

reaching 0.373 GWh by 2030. Meanwhile, TNREP fluctuates, peaking at 0.722 GWh in 2026, then declining to 0.065 GWh by 2029, before rising again to 0.429 GWh in 2030.

Figure 10 illustrates Finland's historical and forecasted TREP, measured in normalized GWh. From 2000 to 2023, the production steadily increased, reaching 1 GWh in 2023. However, projections indicate a slight decline from 2024 to 2030, with values ranging from 0.658 to 0.373 normalized GWh.

Figure 11 shows Finland's TNREP trend from 2000 to 2030 in normalized GWh. The data from 2000 to 2023 show a transition from nonrenewable sources, with a gradual reduction from 0.0415 to 0.2976. The projection from 2024 to 2030 shows unexpected volatility, with values peaking at 0.772 in 2027, falling to 0.065 in 2029, and then increasing to 0.429 by 2030.

4.1.3 | Bi-GRU Model Performance on Data Set of Germany

Figure 12 shows the Bi-GRU model's training and validation loss (MSE) during 100 epochs on the Germany data set. The training loss is considerable initially but quickly drops, suggesting quick learning. The validation loss falls below the training loss at about the 20-epoch point, indicating successful generalization. The model is then shown to be well-tuned and not overfitting by the plateauing of both losses, with the validation loss being somewhat more significant.

Table 9 presents the Bi-GRU model's performance on the Germany testing set with shallow error values, indicating high prediction accuracy. At 0.0017, the MSE indicates that, on average, the model's predictions closely match the actual data. The model's average absolute deviation is reflected in the MAE at 0.0275, which is low and suggests consistency in performance. The model's RMSE of 0.0414 and MAPE of 5.87% indicate that it manages more fantastic mistakes well, guaranteeing dependability across various conditions.

Table 10 shows the normalized output of TREP and TNREP in Germany between 2024 and 2030. The data displays a heterogeneous trend in renewable energy generation, with a noteworthy peak in 2025 (0.674 GWh) and a substantial decline in 2027 (0.209 GWh). There is a peak for nonrenewable energy in 2026 (0.835 GWh), a decline in 2029 (0.405 GWh), and a subsequent increase in 2030 (0.761 GWh).

Figure 13 shows the trend of Germany's total renewable power output from 2000 to 2030. Data from 2022 to 2030 is anticipated, and data from 2000 to 2021 is actual. The graph shows that production increased steadily between 2000 and 2023, when it peaked. After that, there was a significant drop, and the numbers projected for 2024 to 2030 exhibit variations but do not return to the peak of 2023.

Figure 14 illustrates Germany's TNREP from 2000 to 2030, with actual data from 2000 to 2023 and predicted values from 2024 to 2030. Over the observed years, there was a fluctuating trend, with a decline from 2009 to 2020 followed by a peak in 2022. The forecasted values from 2024 to 2030 suggest a gradual rise, peaking around 2026 before stabilizing at relatively higher levels compared to the preceding years.

4.1.4 | Bi-GRU Model Performance on Data Set of Switzerland

The training and validation loss (MSE) of the Bi-GRU model during 100 epochs on the Switzerland data set is displayed in Figure 15. The model learns from the data quickly based on the substantial drop in training loss seen during the first 20 epochs. The training and validation loss curves level off and run almost parallel after this first dip, indicating a steady convergence. Given that there is no discernible difference between the training and validation losses, the two lines' closeness after the training phase suggests that the model generalizes effectively and is not overfitting.

Table 11 presents the Bi-GRU model's performance on the Switzerland testing set, where low error values indicate a

TABLE 8 | Forecasting TREP and TNREP using the Bi-GRU model on the Finland testing set.

Year	Normalized TREP Finland	Normalized TNREP Finland
2024	0.658	0.078
2025	0.442	0.515
2026	0.292	0.722
2027	0.401	0.772
2028	0.668	0.086
2029	0.473	0.065
2030	0.373	0.429

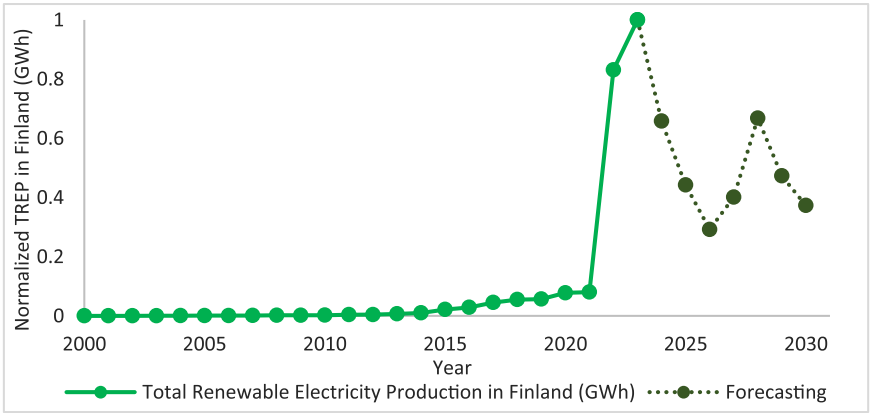

FIGURE 10 | Prediction of TREP in normalized form using the Bi-GRU model on the Finland testing set.

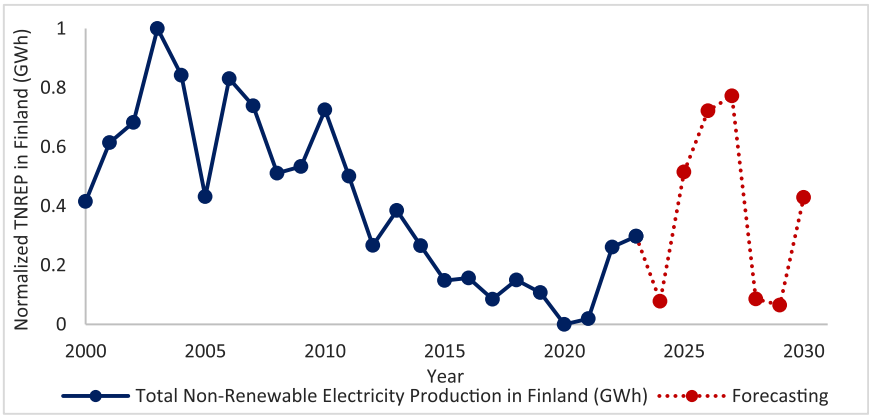

FIGURE 11 | Prediction of TNREP in normalized form using the Bi-GRU model on the Finland testing set.

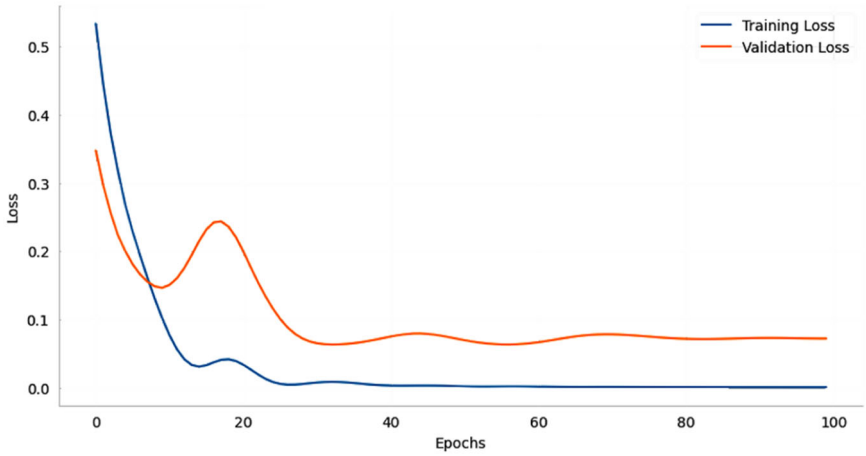

FIGURE 12 | Bi-GRU model's training and validation losses on the Germany data set.

TABLE 9 | Performance of Bi-GRU model on the Germany testing set.

Error description	Error value
MSE	0.0017
MAE	0.0275
RMSE	0.0414
MAPE (%)	5.87

TABLE 10 | Forecasting TREP and TNREP using the Bi-GRU model on the Germany testing set.

Year	Normalized TREP in Germany (GWh)	Normalized TNREP in Germany
2024	0.393	0.56
2025	0.674	0.503
2026	0.503	0.835
2027	0.209	0.745
2028	0.476	0.76
2029	0.636	0.405
2030	0.455	0.761

well-fitting model. The model's accuracy is shown by MSE of 0.0026, while its predictability is indicated by an MAE of 0.0364. The model's ability to control the size of prediction mistakes is indicated by the RMSE of 0.0512, indicating its resilience in real-world settings. Additionally, the MAPE is 2.45%, which measures the average percentage error.

In Table 12, Switzerland's normalized TREP demonstrates varying trends from 2024 to 2030. It starts at 0.577 GWh in 2024, increases to 0.919 GWh in 2026, dips to 0.235 GWh in 2027, reaches a peak of 0.976 GWh in 2029, and stabilizes at 0.722 GWh in 2030.

Meanwhile, normalized TNREP exhibits fluctuations, starting at 0.39 GWh in 2024, dropping to 0.16 GWh in 2026, rising sharply to 0.864 GWh in 2027, declining slightly to 0.517 GWh in 2028, and then climbing to 0.787 GWh in 2030.

Normalized in GWh, Figure 16 shows the trend of Switzerland's total renewable power output from 2000 to 2030. The data reveals a steady increase from negligible amounts in the early 2000s to a significant surge by 2022. From 2024 to 2030, the predicted values suggest fluctuations, with a peak in 2026 followed by a decline. These values are essential for understanding Germany's energy landscape and forecasting future trends in nonrenewable electricity generation.

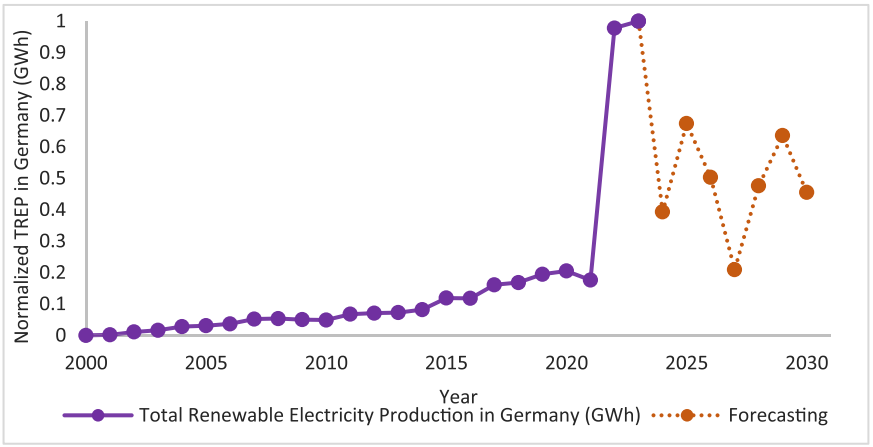

FIGURE 13 | Prediction of TREP in normalized form using the Bi-GRU model on the Germany testing set.

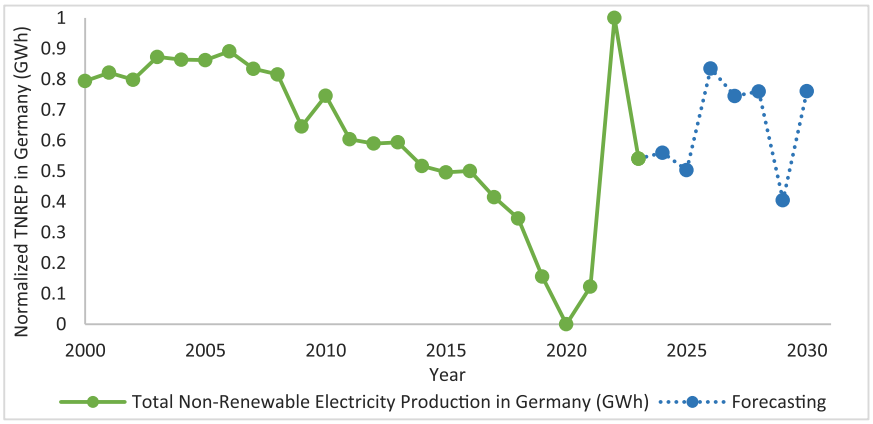

FIGURE 14 | Prediction of TNREP in normalized form using the Bi-GRU model on the Germany testing set.

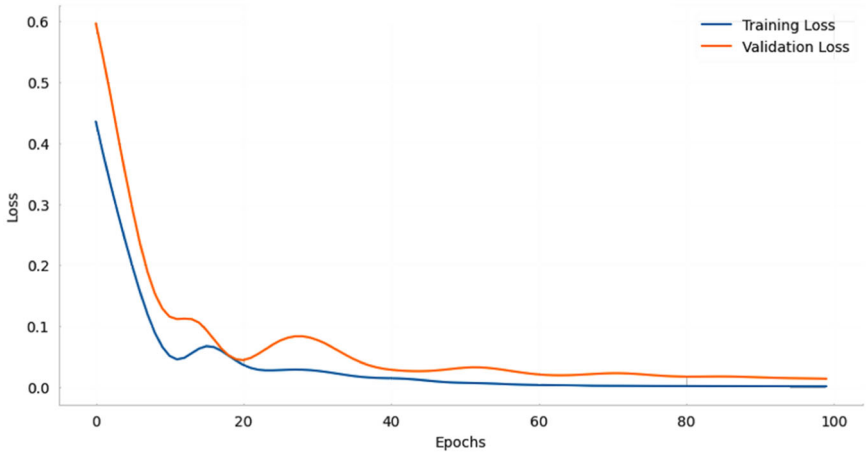

FIGURE 15 | Bi-GRU model's training and validation losses on the Switzerland data set.

Figure 17, normalized in GWh, shows the trend in Switzerland's total nonrenewable power output from 2000 to 2030. Actual values range from 0.165 GWh in 2017 to 1 GWh in 2006, fluctuating over the years. Forecasted values show a decreasing trend from 2024 to 2026, followed by a slight increase and stabilization toward 2030, with projections ranging from 0.16 GWh in 2026 to 0.864 GWh in 2027.

4.2 | Comparison of Deep Learning Models Performance on the Datasets of United Kingdom, Finland, Germany, and Switzerland

Three models are highlighted in Table 13 performance comparison of deep learning models on testing sets from the United Kingdom, Finland, Germany, and Switzerland: Bi-LSTM, CNN

TABLE 11 | Performance of Bi-GRU model on the Switzerland testing set.

Error description	Error value
MSE	0.0026
MAE	0.0364
RMSE	0.0512
MAPE (%)	2.45

TABLE 12 | Forecasting TREP and TNREP using the Bi-GRU model on the Switzerland testing set.

Year	Normalized TREP in Switzerland	Normalized TNREP in Switzerland
2024	0.577	0.39
2025	0.668	0.438
2026	0.919	0.16
2027	0.235	0.864
2028	0.281	0.517
2029	0.976	0.523
2030	0.722	0.787

[35], and an ensemble approach (Bi-LSTM and CNN). Performance metrics include MSE, MAE, and RMSE. The Bi-GRU model indicates that the United Kingdom's MSE, MAE, RMSE, and MAPE are, respectively, 0.0064, 0.034, 0.0797, and 3.79%. The performance parameters of the Bi-GRU in Finland are RMSE: 0.0414, MAE: 0.0275, MSE: 0.0017, and MAPE: 3.17%. Germany's Bi-GRU scores are RMSE: 0.1023, MAE: 0.0475, MSE: 0.0105, and MAPE: 5.87%. Finally, the Bi-GRU model yields the following results for Switzerland: RMSE = 0.0512, MAE = 0.0364, MSE = 0.0026, and MAPE = 2.45%. Finland and Switzerland often have the lowest error rates according to the Bi-GRU model, whereas the Ensemble model best serves the United Kingdom. Errors are often more significant for Germany in all models.

Figure 18 demonstrates that, among the four European nations examined, the Bi-GRU model performed better in terms of MSE, MAE, RMSE, and MAPE than other deep learning models. It has the lowest error metrics among the United Kingdom, Finland, Germany, and Switzerland, suggesting higher prediction accuracy. According to Figure, ensemble approaches and CNN models lag behind the Bi-LSTM model, which is typically the second most accurate model. When comparing the models of the United Kingdom and Germany with those of Finland and Switzerland, the figure shows that the former obtained lower

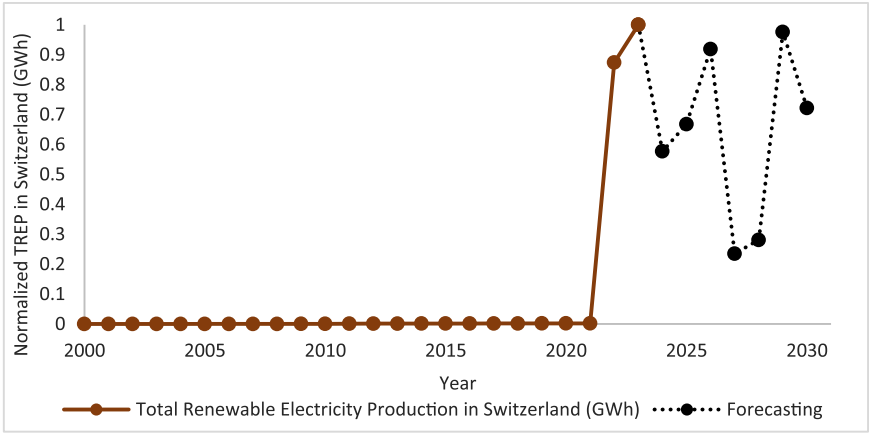

FIGURE 16 | Prediction of TREP in normalized form using the Bi-GRU model on the Switzerland testing set.

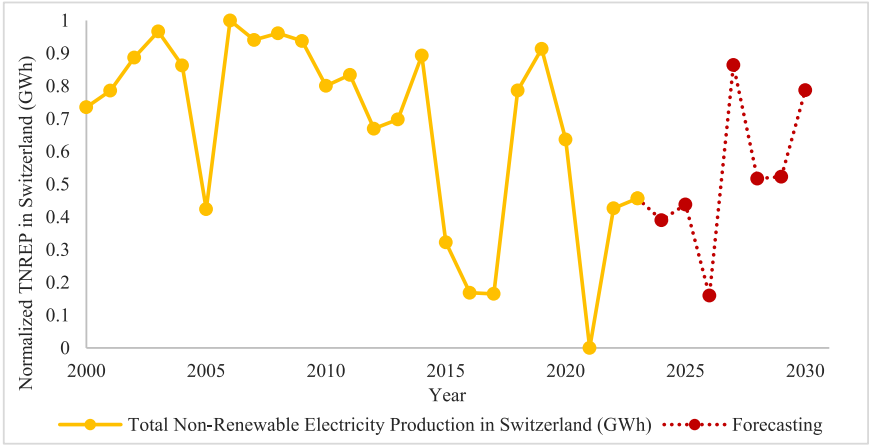

FIGURE 17 | Prediction of TNREP in normalized form using the Bi-GRU model on the Switzerland testing set.

TABLE 13 | Performance comparison of deep learning models on the testing sets of four European countries.

Country	Model	MSE	MAE	RMSE	MAPE (%)
UK	Bi-LSTM	0.0081	0.042	0.0902	5.43
	CNN	0.0101	0.0562	0.1003	7.70
	Ensemble	0.0079	0.0466	0.0886	5.12
	Bi-GRU	**0.0064**	**0.034**	**0.0797**	**3.79**
Finland	Bi-LSTM	0.0021	0.0365	0.0462	6.28
	CNN	0.0059	0.0493	0.0768	4.90
	Ensemble	0.0056	0.0536	0.0747	4.78
	Bi-GRU	**0.0017**	**0.0275**	**0.0414**	**3.17**
Germany	Bi-LSTM	0.012	0.0604	0.1096	7.37
	CNN	0.0135	0.0611	0.1162	8.55
	Ensemble	0.012	0.0615	0.1097	7.35
	Bi-GRU	**0.0105**	**0.0475**	**0.1023**	**5.87**
Switzerland	Bi-LSTM	0.0075	0.059	0.0866	6.05
	CNN	0.0154	0.0905	0.124	8.49
	Ensemble	0.0077	0.0616	0.0877	7.23
	Bi-GRU	**0.0026**	**0.0364**	**0.0512**	**2.45**

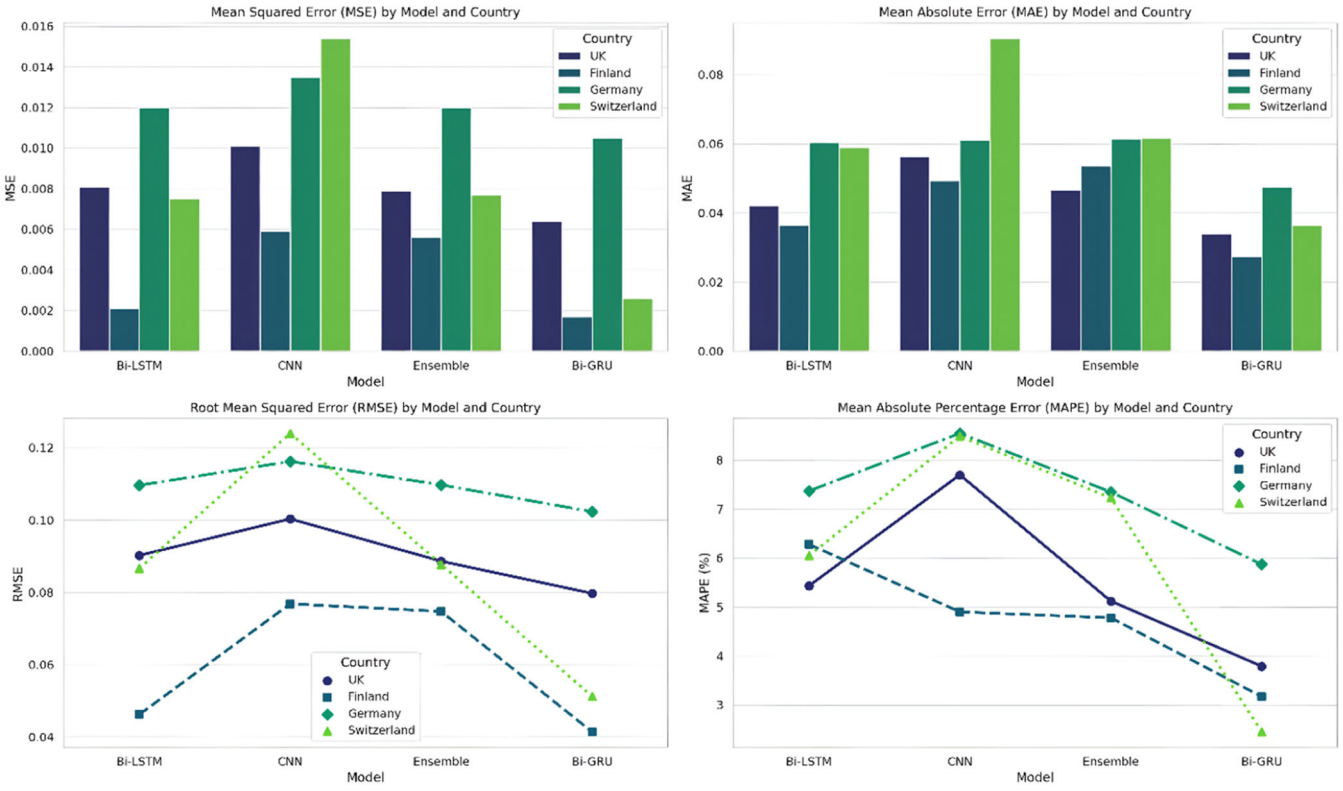

FIGURE 18 | Performance comparison of forecasting models on testing sets of four European countries.

error rates across all criteria. The graph also indicates that ensemble approaches often outperform CNN models and fall short of Bi-LSTM or Bi-GRU models in certain situations.

RMSE is generally higher compared to other error metrics like MAE or MSE because RMSE places greater emphasis on larger errors. RMSE is better at detecting larger outliers since it squares the differences between the actual and predicted values. Since MAE and MSE do not penalize big mistakes to the same degree, a bigger RMSE is normally the outcome of the model sometimes making larger errors, regardless of how infrequent they may be. Data complexity

and the applicability of the model should dictate the RMSE criteria for power generation forecasting. Results for the United Kingdom, Finland, Germany, and Switzerland in the Bi-GRU model demonstrate that an RMSE value below 0.1 is appropriate for guaranteeing model robustness, according to the study. The RMSE values are far lower than what is considered acceptable for energy forecasting applications, especially when taking into account the model's good predicted accuracy and dependability.

4.3 | Ablation Study on European Countries Data Set

Here, we examine the impact of several parameters on the Bi-GRU model's forecast accuracy for renewable and non-renewable electricity output in the United Kingdom, Finland, Germany, and Switzerland (Figure 19). Using RMSE, MAE, MAPE, and MSE, we can quantify the effect of component changes.

4.3.1 | Impact of Bi-GRU Layer Size

Table 14 shows performance metrics (MSE, MAE, RMSE, and MAPE) for a Bi-GRU model with varying layer sizes: 32, 64, and 128 units. The 64-unit model excels, showing the lowest values in MSE (0.0064), MAE (0.034), RMSE (0.079), and MAPE (3.79%), indicating optimal performance among the sizes tested.

4.3.2 | Influence of Feature Scaling

Table 15 compares Bi-GRU model performance using MinMaxScaler and StandardScaler. The MinMaxScaler achieves lower error metrics across MSE (0.0064), MAE (0.034), RMSE (0.079), and MAPE (3.79%), outperforming the StandardScaler, which shows higher values, thereby highlighting its effectiveness in reducing forecast errors.

TABLE 14 | Performance metrics of a Bi-GRU model with different layer sizes.

Layer size (units)	MSE	MAE	RMSE	MAPE (%)
32	0.0089	0.039	0.094	4.85
64	0.0064	0.034	0.079	3.79
128	0.0072	0.038	0.084	3.96

TABLE 15 | Performance of a Bi-GRU model with different scaling techniques.

Scaling method	MSE	MAE	RMSE	MAPE (%)
MinMaxScaler	0.0064	0.034	0.079	3.79
StandardScaler	0.0072	0.036	0.084	4.21

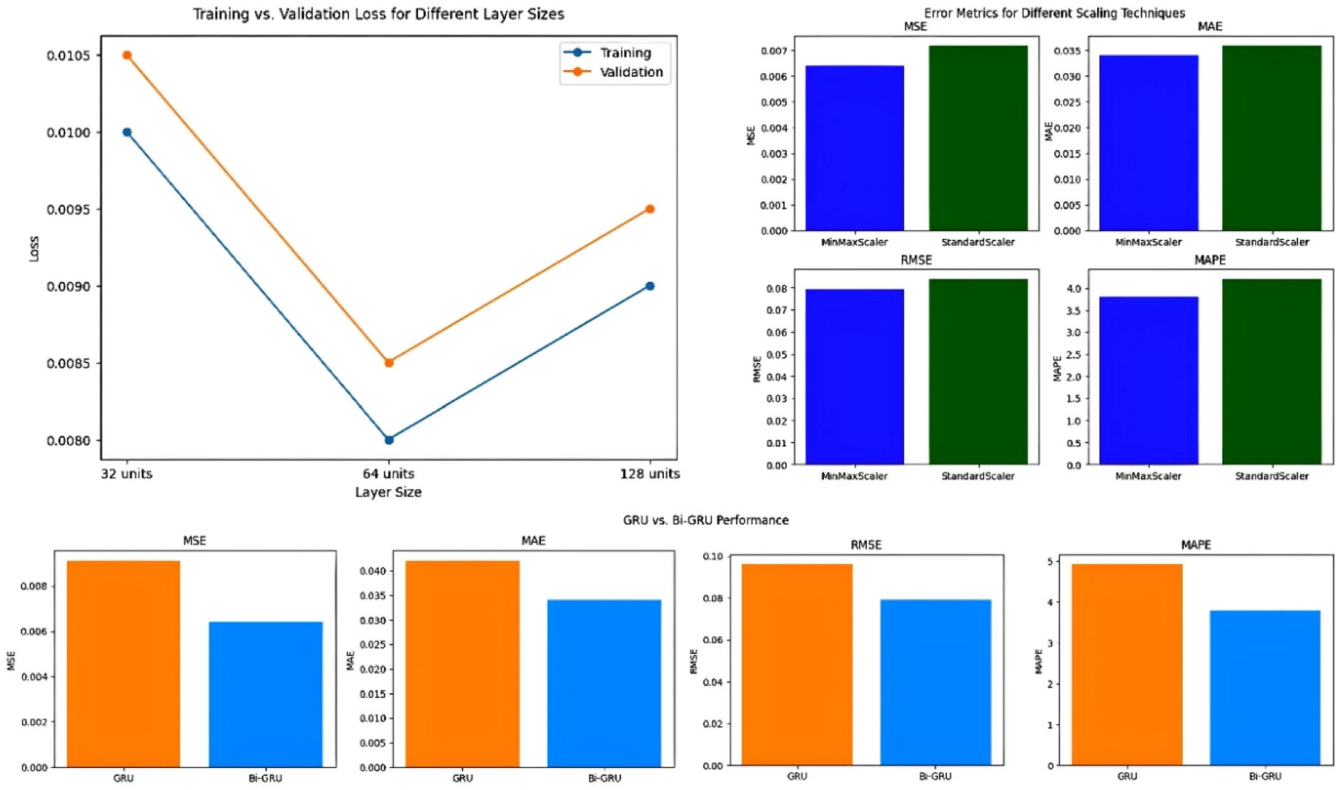

FIGURE 19 | Ablation study on European countries data set.

4.3.3 | Comparison With Single GRU

Table 16 compares the performance of GRU and Bi-GRU models. It shows that the Bi-GRU model achieves lower error rates across all metrics—MSE (0.0064), MAE (0.034), RMSE (0.079), and MAPE (3.79%)—demonstrating its enhanced accuracy in forecasting compared to the GRU model with MSE (0.0091), MAE (0.042), RMSE (0.096), and MAPE (4.92%).

4.4 | Comparison of Bi-GRU Model Performance With Other Existing Studies

Many of the studies being conducted now focus only on renewable energy sources such as solar, wind, and PV electricity. It does not examine how to integrate strategies pertaining to nonrenewable and renewable energy sources. Our study is unique in that it considers both forms of energy. Table 17 compares our data set with other datasets. Nevertheless, no other research has made use of this data set. This comparison demonstrates that there are variations in the volume of data covered and functionalities. Straight comparisons are only feasible if testing procedures and samples vary. In contrast, Table 13 presents the experimental results of other state-of-the-art models applied to the same data set of European countries, allowing for a more relevant comparison. However, Table 17 compares different models used to predict and manage different energy sectors [22]. 's PVMD-ESMA-DELM model only looks at wind power and gets an MAE of 0.9709 and an RMSE of 1.4188. The RNN-LSTM model by [27], which focuses on solar (PV) energy, gives an RMSE value of 19.78. Two models, CNN-LSTM-transformer by Al-Ali et al. [16] and ensemble approach by Mystakidis et al. [19] look at renewable energy in a general way. CNN-LSTM-Transformer has an MAE of 0.393 and an RMSE of 0.344, while Ensemble Approach has an MSE of 3.9972, an MAE of 0.8306, and an RMSE of 1.9993. LightGBM model by Unsal et al. [12] has an MAE of 1.1072 and an RMSE of 1.7479 for green energy. The MLP model by Marques et al. [25] focuses on solar energy and gets an MAE of 0.61 and an RMSE of 1.05. With an MSE of 1.36, the CNN model by Nikulins et al. [20] concentrates on solar and wind energy. The steam energy LSTM model [23] has RMSE of 0.47. The Bi-GRU model analyzes both renewable and nonrenewable energy sources, covering a larger spectrum of energy sources. This model outperforms others in accuracy and efficiency with an MSE of 0.0017, MAE of 0.0275, and RMSE of 0.0414. Since this is a comprehensive approach, the model may be applied to many energy circumstances. Its energy forecast and control method outperforms.

TABLE 16 | Performance of GRU and Bi-GRU models.

Model	MSE	MAE	RMSE	MAPE (%)
GRU	0.0091	0.042	0.096	4.92
Bi-GRU	0.0064	0.034	0.079	3.79

5 | Conclusions and Future Work

This research shows that the Bi-GRU can anticipate European renewable and nonrenewable electricity production. Our comparative analysis reveals that Bi-GRU beats Bi-LSTM, CNN, and Ensemble techniques in prediction accuracy across four European countries (the United Kingdom, Finland, Germany, and Switzerland).

The Bi-LSTM model worked well, although its regional development rates varied for numerous reasons. The United Kingdom's well-established green energy system helped the model find more regular trends, increasing projections. For the same reason, Finland's yearly hydropower peaks were well observed. In contrast, Germany's renewable energy transition has increased energy balance instability and prediction uncertainty. Switzerland's electricity reliance highlights Bi-LSTM's pros and cons. These fluctuations show that models must account for local, seasonal, and energy law variability in energy settings. The primary function of the Bi-GRU model is improving energy production forecasts. For this reason, it's critical to use cutting-edge deep learning methods. Because it is precise and versatile, the Bi-GRU model is a useful tool for energy planning in the future. This is particularly true when demand for sustainable energy rises. The inclusion of economic and climate change aspects in this model will become more crucial as the energy production process gets more complex.

TABLE 17 | Comparison with existing studies.

[Reference], Year	Methodology	MSE	MAE	RMSE
[22], 2022	PVMD-ESMA-DELM	—	0.9709	1.4188
[27], 2022	RNN-LSTM	—	—	19.78
[16], 2023	CNN-LSTM-transformer	—	0.393	0.344
[19], 2023	Ensemble approach	3.9972	0.8306	1.9993
[12], 2024	LightGBM	—	1.1072	1.7479
[20], 2024	CNN	1.36	—	—
[25], 2024	MLP	—	0.61	1.05
[23], 2024	LSTM	—	—	0.47
Proposed model	Bi-GRU model	0.0017	0.0275	0.0414

Mixed models, developed by combining Bi-GRU with other methods, may be used by researchers in the future. More data might be made available to researchers, and prediction accuracy could be enhanced by using these models. The ease of their implementation in other parts of the world depends on how well these types perform in those areas. This study has the potential to be transformed into practical energy management solutions via collaboration with subject matter professionals. Keeping energy system privacy and security intact in the face of rapid technological change is of the utmost importance. We can use these models to provide future energy management systems that are both reliable and efficient. In the future, researchers may focus on big data intelligence and cybersecurity-related issues in various smart grid applications [36–39].

Author Contributions

Javed Rashid: investigation, formal analysis, resources, supervision, writing–review and editing. **Sajjad Ahmad:** data curation, formal analysis, investigation, resources, validation, writing–original draft. **Muhammad S. Saleem:** conceptualization, methodology, software, visualization, writing–original draft. **Muhammad Faheem:** data curation, investigation, software, validation, writing–review and editing. **Yonghong Liu:** data curation, investigation, software, validation, writing–review and editing.

Acknowledgments

The authors thank their affiliated universities for providing research facilities.

Ethics Statement

The authors have nothing to report.

Consent

The authors have nothing to report.

Conflicts of Interest

The authors declare no conflicts of interest.

Data Availability Statement

The data will be available upon request to the corresponding author.

References

1. W. Strielkowski, L. Civín, E. Tarkhanova, M. Tvaronavičienė, and Y. Petrenko, "Renewable Energy in the Sustainable Development of Electrical Power Sector: A Review," *Energies* 14, no. 24 (2021): 8240.

2. B. Freedman, "Renewable and Non-Renewable Energy Sources," *Environmental Science* 11, no. 5 (2024): 32016.

3. "National Grid," accessed April 07, 2024, https://www.nationalgrid.com/stories/energy-explained/how-much-uks-energy-renewable.

4. "Finland: Power Production Share by Source 2023," accessed April 08, 2024, https://www.statista.com/statistics/1235401/finland-distribution-of-electricity-production-by-source/.

5. "Public Electricity Generation in Germany 2023," accessed April 07, 2024, https://www.ise.fraunhofer.de/en/press-media/press-releases/2024/public-electricity-generation-2023-renewable-energies-cover-the-majority-of-german-electricity-consumption-for-the-first-time.html.

6. M. Faheem, B. Raza, M. S. Bhutta, and S. H. H. Madni, "A Blockchain-Based Resilient Andsecure Framework for Events Monitoring and Control Indistributed Renewable Energy Systems," *IET Blockchain* 6 (2024): 1–15, https://doi.org/10.1049/blc2.12081.

7. M. Faheem, M. A. Al-Khasawneh, A. A. Khan, and S. H. H. Madni, "Cyberattack Patterns in Blockchain-Based Communication Networks for Distributed Renewable Energy Systems: A Study on Big Datasets," *Data in Brief* 53, no. 4 (2024): 110212, https://doi.org/10.1016/j.dib.2024.110212.

8. S. Reza, M. C. Ferreira, J. J. M. Machado, and J. M. R. S. Tavares, "A Customized Residual Neural Network and Bi-Directional Gated Recurrent Unit-Based Automatic Speech Recognition Model," *Expert Systems With Applications* 215 (2023): 119293.

9. M. Faheem and M. A. Al-Khasawneh, "Multilayer Cyberattacks Identification and Classification Using Machine Learning in Internet of Blockchain (IoBC)-Based Energy Networks," *Data in Brief* 54, no. 3 (2024): 110461, https://doi.org/10.1016/j.dib.2024.110461.

10. S. Zeng, Z. Zhang, X. Cheng, X. Cai, M. Cao, and W. Guo, "Prediction of Soluble Solids Content Using Near-Infrared Spectra and Optical Properties of Intact Apple and Pulp Applying Plsr and CNN," *Spectrochimica Acta, Part A: Molecular and Biomolecular Spectroscopy* 304 (2024): 123402.

11. D. Venkateswaran and Y. Cho, "Efficient Solar Power Generation Forecasting for Greenhouses: A Hybrid Deep Learning Approach," *Alexandria Engineering Journal* 91 (2024): 222–236.

12. D. B. Unsal, A. Aksoz, S. Oyucu, J. M. Guerrero, and M. Guler, "A Comparative Study of AI Methods on Renewable Energy Prediction for Smart Grids: Case of Turkey," *Sustainability* 16, no. 7 (2024): 2894.

13. S. Cen and C. G. Lim, "Multi-Task Learning of the Patchtcn-TST Model for Short-Term Multi-Load Energy Forecasting Considering Indoor Environments in a Smart Building," *IEEE Access* 12 (2024): 19553–19568.

14. A. Motwakel, "Predictive Multimodal Deep Learning-Based Sustainable Renewable and Non-Renewable Energy Utilization," *Computer Systems Science and Engineering* 47, no. 1 (2023): 1267–1281.

15. B. Predić, L. Jovanovic, V. Simic, et al., "Cloud-Load Forecasting via Decomposition-Aided Attention Recurrent Neural Network Tuned by Modified Particle Swarm Optimization," *Complex & Intelligent Systems* 10, no. 2 (2024): 2249–2269.

16. E. M. Al-Ali, Y. Hajji, Y. Said, et al., "Solar Energy Production Forecasting Based on a Hybrid CNN-LSTM-Transformer Model," *Mathematics* 11, no. 3 (2023): 676.

17. A. Alrasheedi and A. Almalaq, "Hybrid Deep Learning Applied on Saudi Smart Grids for Short-Term Load Forecasting," *Mathematics* 10, no. 15 (2022): 2666.

18. T. Anu Shalini and B. Sri Revathi, "Hybrid Power Generation Forecasting Using CNN Based BILSTM Method for Renewable Energy Systems," *Automatika* 64, no. 1 (2023): 127–144.

19. A. Mystakidis, E. Ntozi, K. Afentoulis, et al., "Energy Generation Forecasting: Elevating Performance With Machine and Deep Learning," *Computing* 105, no. 8 (2023): 1623–1645.

20. A. Nikulins, K. Sudars, E. Edelmers, et al., "Deep Learning for Wind and Solar Energy Forecasting in Hydrogen Production," *Energies* 17, no. 5 (2024): 1053.

21. D. Kumar, H. D. Mathur, S. Bhanot, and R. C. Bansal, "Forecasting of Solar and Wind Power Using LSTM RNN for Load Frequency Control in Isolated Microgrid," *International Journal of Modelling and Simulation* 41, no. 4 (2021): 311–323.

22. G. An, L. Chen, J. Tan, Z. Jiang, Z. Li, and H. Sun, "Ultra-Short-Term Wind Power Prediction Based on PVMD-ESMA-DELM," *Energy Reports* 8 (2022): 8574–8588.

23. M. Pasandideh, M. Taylor, S. R. Tito, M. Atkins, and M. Apperley, "Predicting Steam Turbine Power Generation: A Comparison of Long Short-Term Memory and Willans Line Model," *Energies* 17, no. 2 (2024): 352.

24. A. P. Wibawa, A. F. Fadhilla, A. K. A. I. Paramarta, et al. 2024. "Bidirectional Long Short-Term Memory (Bi-LSTM) Hourly Energy Forecasting," In *E3S Web of Conferences* (Vol. 501, p. 01023). EDP Sciences.

25. A. L. F. Marques, M. J. Teixeira, F. V. De Almeida, and P. L. P. Corrêa, "Neural Networks Forecast Models Comparison for the Solar Energy Generation in Amazon Basin," *IEEE Access* 12 (2024): 17915–17925.

26. M. Abubakar, Y. Che, M. Faheem, M. S. Bhutta, and A. Q. Mudasar, "Intelligent Modeling and Optimization of Solar Plant Production Integration in the Smart Grid Using Machine Learning Models," *Advanced Energy and Sustainability Research* 5 (2024): 2300160.

27. M. N. Akhter, S. Mekhilef, H. Mokhlis, et al., "An Hour-Ahead PV Power Forecasting Method Based on an RNN-LSTM Model for Three Different PV Plants," *Energies* 15, no. 6 (2022): 2243.

28. "Dataset of Renewable and Non-Renewable Electricity Production From 2000 to 2021," accessed April 07, 2024, https://climatedata.imf.org/pages/access-data.

29. "Dataset of Renewable and Non-Renewable Electricity Production From 2022 to 2023," accessed April 07, 2024, https://ember-climate.org/.

30. F. T. Lima and V. M. A. Souza, "A Large Comparison of Normalization Methods on Time Series," *Big Data Research* 34 (2023): 100407.

31. P. Mohammadi, A. Rashidi, M. Malekzadeh, and S. Tiwari, "Evaluating Various Machine Learning Algorithms for Automated Inspection of Culverts," *Engineering Analysis With Boundary Elements* 148 (2023): 366–375.

32. A. Mystakidis, E. Ntozi, K. Afentoulis, et al., "Energy Generation Forecasting: Elevating Performance With Machine and Deep Learning," *Computing* 105 (2023): 1623–1645.

33. S. I. Alma'asfa, F. Y. Fraige, M. S. Abdul Aziz, C. Y. Khor, and L. A. Al-Khatib, "Evaluating the Performance of the Anwaralardh Photovoltaic Power Generation Plant in Jordan: Comparative Analysis Using Artificial Neural Networks and Multiple Linear Regression Modeling," *International Journal of Renewable Energy Development* 13, no. 4 (2024): 608–617.

34. "Welcome to Colaboratory," accessed April 01, 2024, https://colab.research.google.com/notebooks/intro.ipynb?utm_source%20=%20scs-index.

35. A. Pourdaryaei, M. Mohammadi, H. Mubarak, et al., "A New Framework for Electricity Price Forecasting via Multi-Head Self-Attention and CNN-Based Techniques in the Competitive Electricity Market," *Expert Systems With Applications* 235 (2024): 121207.

36. M. Faheem, H. Kuusniemi, B. Eltahawy, M. S. Bhutta, and B. Raza, "'A Lightweight Smartcontracts Framework for Blockchain-Based Securecommunication in Smart Grid Applications'," *IET Generation, Transmission and Distribution* 18 (2024): 625–638, https://doi.org/10.1049/gtd2.13103.

37. B. Raza, A. Aslam, A. Sher, A. Kamran Malik, and M. Faheem, "'Autonomic Performance Prediction Framework for Data Warehouse Queries Using Lazy Learning Approach'," *Applied Soft Computing* 91 (2020): 106216.

38. M. A. S. Al-Khasawneh, M. Faheem, E. A. Aldhahri, A. Alzahrani, and A. A. Alarood, "'A MapReduce Based Approach for Secure Batch Satellite Image Encryption'," *IEEE Access* 11, no. 5 (2023): 62865–62878, https://doi.org/10.1109/ACCESS.2023.3279719.

39. M. Faheem, S. B. Hussain Shah, R. Aslam Butt, et al., "'Smart Grid Communication and Information Technologies in the Perspective of Industry 4.0: Opportunities and Challenges'," *Computer Science Review* 30 (2018): 1–30.